Measuring the Relative Strengths and Phases of a Set of Partially Coherent Sources

by

Hidechito HAYASHI* and M. J. Fisher**

The measurement of the characteristics of the acoustic field generated by a set of sources is very important to understand and to control the noise.

In the 1970's, M. J. Fisher proposed the Polar Correlation Technique[1] to solve this problem. The Polar Correlation Technique and the development of it[2] indicate the relationship between the cross spectra measured in the acoustical far field and the distribution of source strengths. And it is proposed the method of a least squares error of cross spectra to estimate the source strength distribution at the case of aero-engine accurately. In the last report[3] it is extended this method for the relative strengths of partially coherent sources. The results of this method was better than that with the direct calculating method.

In the present work it is extended this method for the case of unknown characteristics not only the relative strength but also the phase between the array of partially coherent sources.

1. INTRODUCTION

It is important to estimate the characteristics of noise source array for the noise control technics. The Polar Correlation Technique[1] and the development of it[2] made to estimate the source strength distribution with the cross spectra of microphones located on a polar arc in the acoustical far field. Assuming that the positions of sources are known, the sources strengths are calculated by using a least squares fit procedure of measured cross-spectra data. The original technique is restricted to the case of the mutually incoherent sources. But in the reference[3], it was extended to apply the partially coherent sources with introducing several reference microphones. It can estimate the strengths of interacting noise sources.

However it is restricted only the case of the phase differences in relating to the convection velocity of turbulence being known between each two sources.

In this report we estimate the relative strengths and the phase of the noise source array when the positions of sources are only known for monopole sources.

Received on April 24, 1997

*Department of Mechanical Systems Engineering.
**ISVR, University of Southampton (U. K.)

2. Modeling of measuring system

2.1 Setting the microphones

Figure 1 shows the model of the noise source array and the microphone array. All noise sources are the monopole and fluctuate with the convection velocity Uc. Some of the sources have partially coherent each other. The microphone array follows to the Polar Correlation technique[1], that is, set the arc positions at the radius r_0 from the center of the nozzle outlet. The cross spectra of two signals from microphones are measured.

The cross spectrum between microphones m and n in the far field noise can be written

$$C(m,n)=\sum_k \sum_l \frac{a_k \cdot a_l \cdot c_{kl} \cdot \exp\left(j \cdot \omega \frac{r_{km}-r_{ln}}{a_0}\right)}{r_{km}-r_{ln}} \qquad (2.1)$$

where a_k and a_l are the strength of the noise source k and l, c_{kl} is the complex correlation coefficient between source k and l which includes the phase difference caused by the convecting turbulence velocity U_c. r_{km} and r_{ln} are the distance from the source k to

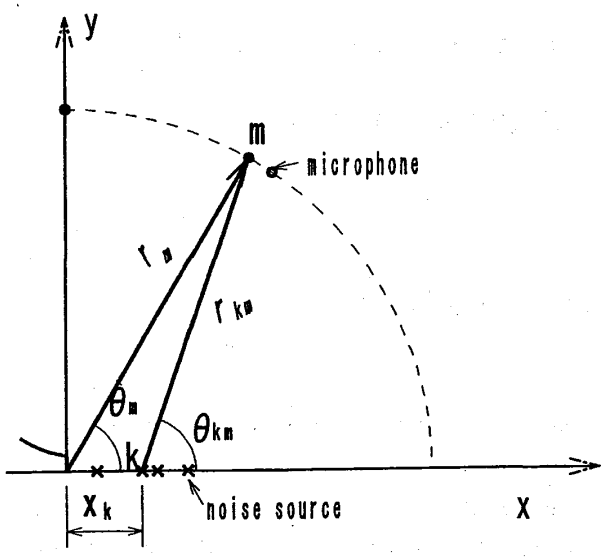

Fig. 1 Model Geometry

microphone m and l to n, respectively.

Now put the term of $a_k \cdot a_l \cdot a_{kl}$ to the complex cross spectrum coefficient b_{kl}.

$$b_{kl}=a_k \cdot a_l \cdot c_{kl} \tag{2.2}$$

then

$$b_{kl}=bR_{kl}+j \cdot bI_{kl} \tag{2.3}$$

where bR_{kl} is the real part and bl_{kl} is the imaginary part of b_{kl}.

Thus the equation (2.1) is rewritten as follows,

$$C(m, n)=\sum_k \sum_l \frac{(bR_{kl}+j \cdot bI_{kl}) \cdot \exp j \cdot \phi_{mnkl}}{r_{km} \cdot r_{ln}} \tag{2.4}$$

where $j \cdot \phi_{mnkl}$ is the phase of cross spectrum caused by the difference of propagation time of noise and is obtained previously by geometric relations between microphones and noise sources.

$$\phi_{mnkl}=\omega \frac{r_{km}-r_{ln}}{a_0} \tag{2.5}$$

A set of the cross spectral $C(m,n)$ measured at the arc microphone array in far field determines the complex cross spectrum coefficients by using the least squares fit method.

2.2 The Least squares fitting method

Fitting the least square method[2] for the cross spectral $C(m,n)$, the error is revealed as follows,

$$\begin{aligned}\sigma^2 &=\frac{1}{M}\frac{1}{N}\sum_m \sum_n \left| \tilde{C}(m, n)-C(m, n) \right|^2 \\ &=\frac{1}{M}\frac{1}{N}\sum_m \sum_n \{\tilde{C}(m, n)-C(m, n)\} \\ &\quad \cdot \overline{\{\tilde{C}(m, n)-C(m, n)\}}\end{aligned} \tag{2.6}$$

where $\tilde{C}(m, n)$ is the measured values and consists with the real $\tilde{R}(m, n)$ and imaginary $\tilde{I}(m, n)$ parts.

The upper bar of the second term of right hand side is the conjugate value of complex.

Thus this conjugate term may be written,

$$\begin{aligned}&\overline{\{\tilde{C}(m, n)-C(m, n)\}}=\overline{\tilde{C}(m, n)}-\overline{C(m, n)} \\ &=\{\tilde{R}(m, n)-j \cdot \tilde{I}(m, n)\} \\ &\quad -\sum_k \sum_l \frac{(bR_{kl}-j \cdot bI_{kl}) \cdot \exp(-j \cdot \phi_{mnkl})}{r_{km} \cdot r_{ln}}\end{aligned} \tag{2.7}$$

And the error is written as,

$$\begin{aligned}\sigma^2 &=\frac{1}{M}\frac{1}{N}\sum_m \sum_n \\ &\left[\{\tilde{R}(m, n)+j \cdot \tilde{I}(m, n)\}\right. \\ &\quad \left.-\sum_k \sum_l \frac{(bR_{kl}+j \cdot bI_{kl}) \cdot \exp(+j \cdot \phi_{mnkl})}{r_{km} \cdot r_{ln}}\right] \\ &\cdot\left[\{\tilde{R}(m, n)-j \cdot \tilde{I}(m, n)\}\right. \\ &\quad \left.-\sum_k \sum_l \frac{(bR_{kl}-j \cdot bI_{kl}) \cdot \exp(-j \cdot \phi_{mnkl})}{r_{km} \cdot r_{ln}}\right]\end{aligned} \tag{2.8}$$

To find the minimum error,

$$\frac{\partial \sigma^2}{\partial bR_{pq}}=0, \quad \frac{\partial \sigma^2}{\partial bI_{pq}}=0 \tag{2.9}$$

Then insertion of equation (2.8) to equation (2.9) yields

$$\begin{aligned}&\frac{1}{M}\frac{1}{N}\sum_m \sum_n \left(\frac{\tilde{R} \cdot \cos\phi_{mnpq}}{r_{pm} \cdot r_{qn}}+\frac{\tilde{I} \cdot \sin\phi_{mnpq}}{r_{pm} \cdot r_{qn}}\right) \\ &\quad =\sum_k \sum_l bR_{kl} \cdot \frac{1}{M}\frac{1}{N}\sum_m \sum_n \frac{\cos(\phi_{mnpq}-\phi_{mnkl})}{r_{pm} \cdot r_{qn} \cdot r_{km} \cdot r_{ln}} \\ &\quad +\sum_k \sum_l bl_{kl} \cdot \frac{1}{M}\frac{1}{N}\sum_m \sum_n \frac{\sin(\phi_{mnpq}-\phi_{mnkl})}{r_{pm} \cdot r_{qn} \cdot r_{km} \cdot r_{ln}} \\ &\frac{1}{M}\frac{1}{N}\sum_m \sum_n \left(\frac{\tilde{R} \cdot \sin\phi_{mnpq}}{r_{pm} \cdot r_{qn}}-\frac{\tilde{I} \cdot \cos\phi_{mnpq}}{r_{pm} \cdot r_{qn}}\right) \\ &\quad =\sum_k \sum_l bR_{kl} \cdot \frac{1}{M}\frac{1}{N}\sum_m \sum_n \frac{\sin(\phi_{mnpq}-\phi_{mnkl})}{r_{pm} \cdot r_{qn} \cdot r_{km} \cdot r_{ln}} \\ &\quad -\sum_k \sum_l bl_{kl} \cdot \frac{1}{M}\frac{1}{N}\sum_m \sum_n \frac{\cos(\phi_{mnpq}-\phi_{mnkl})}{r_{pm} \cdot r_{qn} \cdot r_{km} \cdot r_{ln}}\end{aligned} \tag{2.10}$$

In both equations the left hand sides comprise a set of measured data and the geometric relation between the sources and the microphones. The right hand sides comprise the source correlation coefficients and the geometric relations. Replace the upper equations for each pair of (p,q) values,

$$\begin{aligned}\tilde{MR}(p, q) &=\sum_k \sum_l (bR_{kl} \cdot HRR(p, q, k, l)) \\ &\quad +\sum_k \sum_l (bI_{kl} \cdot HRR(p, q, k, l)) \\ \tilde{MI}(p, q) &=\sum_k \sum_l (bR_{kl} \cdot HIR(p, q, k, l)) \\ &\quad +\sum_k \sum_l (bI_{kl} \cdot HIR(p, q, k, l))\end{aligned} \tag{2.11}$$

where

$$\tilde{MR}(p,\ q)=\frac{1}{M}\frac{1}{N}\sum_m\sum_n\left(\frac{\tilde{R}\cdot\cos\phi_{mnpq}}{r_{pm}\cdot r_{qn}}+\frac{\tilde{I}\cdot\sin\phi_{mnpq}}{r_{pm}\cdot r_{qn}}\right)$$

$$\tilde{MI}(p,\ q)=\frac{1}{M}\frac{1}{N}\sum_m\sum_n\left(\frac{\tilde{R}\cdot\sin\phi_{mnpq}}{r_{pm}\cdot r_{qn}}+\frac{\tilde{I}\cdot\cos\phi_{mnpq}}{r_{pm}\cdot r_{qn}}\right)$$

$$HRR(p,\ q,\ k,\ l)=\frac{1}{M}\frac{1}{N}\sum_m\sum_n\frac{\cos(\phi_{mnpq}-\phi_{mnkl})}{r_{pm}\cdot r_{qn}\cdot r_{km}\cdot r_{ln}}$$

$$HRI(p,\ q,\ k,\ l)=\frac{1}{M}\frac{1}{N}\sum_m\sum_n\frac{\sin(\phi_{mnpq}-\phi_{mnkl})}{r_{pm}\cdot r_{qn}\cdot r_{km}\cdot r_{ln}}$$

$$HIR(p,\ q,\ k,\ l)=\frac{1}{M}\frac{1}{N}\sum_m\sum_n\frac{\sin(\phi_{mnpq}-\phi_{mnkl})}{r_{pm}\cdot r_{qn}\cdot r_{km}\cdot r_{ln}}$$
$$=HRI(p,\ q,\ k,\ l)$$

$$HII(p,\ q,\ k,\ l)=-\frac{1}{M}\frac{1}{N}\sum_m\sum_n\frac{\cos(\phi_{mnpq}-\phi_{mnkl})}{r_{pm}\cdot r_{qn}\cdot r_{km}\cdot r_{ln}}$$
$$=-HRR(p,\ q,\ k,\ l) \tag{2.12}$$

where $MR(p,q)$, $\tilde{MI}(p,q)$ are the vectors from measured cross spectra. $HRR(p,q,k,l)$, $HRI(p,q,k,l)$, $HIR(p,q,k,l)$, and $HII(p,q,k,l)$ are elements of the geometric matrix H.

$$H=\begin{pmatrix}HRR & HRI\\ HIR & HII\end{pmatrix} \tag{2.13}$$

Hence in matrix notation

$$\begin{pmatrix}\tilde{MR}\\ \tilde{MI}\end{pmatrix}=H\cdot\begin{pmatrix}BR\\ BI\end{pmatrix},\quad \begin{matrix}BR=(bR_{pq})\\ BI=(bI_{pq})\end{matrix} \tag{2.14}$$

In the above equation the left hand side vector consists of $2\times K$ dimension, the geometric matrix of right hand side of $(2\times K)^2$ and the complex cross spectral coefficient vector of $2\times K$. From equation (2.14) we can solve the (bR,bI). In this report, we use the Gaussian elimination method.

3. Estimation of convecting disturbance velocity

From the above method, we can get the complex correlation coefficients (bR,bI). These complex values contain the relative source strength and the phase differences of each source. The phase difference is revealed by the following equation.

$$\Psi_{kl}=\omega\frac{x_k-x_l}{Uc} \tag{3.1}$$

where Ψ_{kl} is the phase difference of source k and l, x_k,x_l are positions of source k and l, and U_c is the convecting disturbance velocity. This equation indicates that the phase difference is caused by the ratio of the distance of sources and the convecting disturbance velocity. From this equation the convecting disturbance velocity U_c can be related to the phase difference. But the phase has the periodicity of 2π so the convecting disturbance velocity can not be calculated uniquely from equation (3.1).

In this paper we propose the method to calculate the convecting disturbance velocity from the complex correlation coefficients of sources. At a angular velocity ω, the complex correlation coefficient b_{kl} between source k and l, can be written as following equation from equation (2.3),

$$b_{kl}=bR_{kl}+j\cdot bI_{kl}=bmag(\omega)\cdot\exp(j\cdot\Psi_{kl})$$
$$=bmag(\omega)\cdot\exp\left(j\cdot\omega\frac{x_k-x_l}{U_c}\right) \tag{3.2}$$

Now we differentiate this equation by ω,

$$\frac{db_{kl}}{d\omega}=\left(\frac{dbmag(\omega)}{d\omega}+j\cdot bmag(\omega)\frac{x_k-x_l}{U_c}\right)$$
$$\cdot\exp\left(j\cdot\omega\frac{x_k-x_l}{U_c}\right) \tag{3.3}$$

The left hand side is the differential of db_{kl} with ω, this can be rewritten by the differential of real and imaginary parts.

$$\frac{db_{kl}}{d\omega}=\frac{dbR_{kl}}{d\omega}+j\frac{dbI_{kl}}{d\omega} \tag{3.4}$$

we use the fourth accuracy numerical differential technique. A real part and an imaginary part are obtained with following equations by using the estimated correlation coefficients for each real and imaginary parts.

$$\frac{dbR_{kl}}{d\omega}=\frac{8\cdot\{bR_{kl}(\omega+d\omega)-bR_{kl}(\omega-d\omega)\}}{12\cdot d\omega}$$
$$-\frac{\{bR_{kl}(\omega+2\,d\omega)-bR_{kl}(\omega-2\,d\omega)\}}{12\cdot d\omega}$$
$$\frac{dbI_{kl}}{d\omega}=\frac{8\cdot\{bI_{kl}(\omega+d\omega)-bI_{kl}(\omega-d\omega)\}}{12\cdot d\omega}$$
$$-\frac{\{bI_{kl}(\omega+2\,d\omega)-bI_{kl}(\omega-2\,d\omega)\}}{12\cdot d\omega} \tag{3.5}$$

The each term in the parenthesis of the right hand of equation (3.3) is obtained from using equation (3.2) as follows.

$$\frac{dbmag}{d\omega}=Re\left[\left(\frac{dbR_{kl}}{d\omega}+j\frac{dbI_{kl}}{d\omega}\right)\cdot\exp(-j\cdot\Psi_{kl})\right]$$
$$bmag\frac{x_k-x_l}{U_c}=Im\left[\left(\frac{dbR_{kl}}{d\omega}+j\frac{dbI_{kl}}{d\omega}\right)\cdot\exp(-j\cdot\Psi_{kl})\right] \tag{3.6}$$

where the phase and the magnitude are obtained from next equations,

$$\Psi_{kl}=\tan^{-1}\frac{bI_{kl}}{bR_{kl}},\quad bmag=\sqrt{bR_{kl}^2+bI_{kl}^2} \tag{3.7}$$

We have to notice that the complex correlation values b_{kl} have some errors and it needs to be adopted the statistic treatment, that is, least square fitting method. From equation (3.3), (3.5) to (3.7) we obtain the following equation by using the weighted average to U_c.

$$U_c=\sum_k\sum_l\Big[(x_k-x_l)\cdot bmag \cdot\mathrm{Im}\Big\{\Big(\frac{dbR_{kl}}{d\omega}+j\frac{dbI_{kl}}{d\omega}\Big)\exp(-j\cdot\Psi_{kl})\Big\}\cdot fw_{kl}\Big]\Big/ \sum_k\sum_l\Big[\mathrm{Im}\Big\{\Big(\frac{dbR_{kl}}{d\omega}+j\frac{dbI_{kl}}{d\omega}\Big)\exp(-j\cdot\Psi_{kl})\Big\}^2\cdot fw_{kl}\Big] \tag{3.8}$$

where fw_{kl} is the weighted function and in this case it is as same as the magnitude of complex correlation coefficient.

4. Example of numerical simulation

4.1 Simulated sources and microphone array

The numerical simulation model was the same as the case of reference[2]. The shock cell noise was generated from the supersonic jet blown from a 50 mm diameter nozzle. Six shock cells were set at 50 mm intervals. Shock cells interacted with the shear flow and generated point monopole noises. The convecting disturbance velocity U_c was assumed to be 250 m/s. This velocity was used to set the complex cross spectra. The mutual coherence of sources were arranged, 0.75 between source n and $n\pm1$, 0.5 between n and $n\pm2$, 0.25 between n and $n\pm3$, and zero between n and $n\pm4$, and beyond. The far field microphone array situated around an arc of 10 m radius from the nozzle outlet. The angle of array covered the range of 61 to 90 degree from the nozzle axis. The two cases of microphone array were tested, the one was at 30 microphone array in 1 degree intervals and the another was at 6 microphone array with 6 degree interval. The sound speed was taken as 342 m/s.

4.2 Calculating condition

At first we generated the cross spectra with the following equation. It included the phase difference induced by the convecting disturbance. But when the noise source characteristics was solved from a set of these cross spectra, the value of this phase difference is not used, but is obtained as a part of results of complex cross spectrum coefficients.

$$C(m,n)=\sum_k\sum_l\frac{a_k\cdot a_l\cdot c_{kl}\cdot\exp\Big\{j\cdot\omega\Big(\frac{r_{km}-r_{ln}}{a_0}+\frac{x_k-x_l}{U_c}\Big)\Big\}}{r_{km}\cdot r_{ln}} \tag{4.1}$$

As mentioned above, the microphones were set with equally intervals. The angle of intervals Δ was in 1 degree or 6 degree. The angle of mth microphone α_m is put as follows,

$$\sin\alpha_m=m\cdot\sin\Delta \tag{4.2}$$

This angle referenced to the normal of the nozzle axis. The distance r_{pm} between the noise source number p and the microphone number m, and the phase difference ϕ_{mnpq} of noise source number p and q and microphone number m and n are written,

$$r_{pm}=r_0-x_p\cdot\sin\alpha_m=r_0-x_p\cdot\sin\Delta$$
$$\phi_{mnpq}=\omega\frac{r_{pm}-r_{qn}}{a_0}=\omega\frac{x_q\cdot n\cdot\sin\Delta-x_p\cdot m\cdot\sin\Delta}{a_0} \tag{4.3}$$

4.3 Statistical condition in far field cross spectra

In an actual measurement, some kinds of uncertainty include in the output of data; the radius positioning uncertainty of microphones from the nozzle outlet, the angle uncertainty of microphone arranged angles and the output uncertainty of signal from microphones. In order to simulate this uncertainty in the computer, the probability random noise are added in calculating the cross spectra.

The statistical uncertainty of the radius position would make to generate the errors of magnitude and the phase difference in cross spectra. In the numerical simulation, we add the statistical errors of the radius position of microphone in generating the cross spectra. The radius r_0' added the statistical error is put as following equation,

$$r_0'=r_0\cdot\Big(1+\frac{e_r\times rand}{100}\Big) \tag{4.4}$$

where e_r is the specified percentage of radius positioning error and *'rand'* is a probability number between -1 to 1.

The statistical uncertainty of arranged angle would mainly cause the error of phase difference in cross spectra. As same as the radius positioning error generation, the position of microphone added the statistical angle error is put as following equation,

$$r_{km}' = r_0 - x_k \cdot \left(m \cdot \sin\Delta + \frac{e_a \cdot rand}{100} \sin\Delta \right) \qquad (4.5)$$

where e_a is the specified percentage of arranged angle error.

The statistical uncertainty of microphone output in cross spectra is added to the calculated cross spectra. The error noise is added to real and imaginary parts of cross spectra. This technics is same as the reference (3),

$$AddedNoise = \frac{e \times rand}{100} \sum_k \frac{a_k^2}{r_0^2} \qquad (4.6)$$

where e are the specified percentage of noise error.

5. Theoretical treatment

At low frequencies the variation of the cosine and sine function in equation (2.12) becomes small with the microphone number variation. Then the discrete values summation in equation (2.12) can be replaced by the integrals in relation to the microphone number m and n. In this case, we put the following approximation, the noise source distance x is very small compare to the distance between the microphone and the nozzle outlet r_0; $r_0 >> x \cdot \sin\alpha$.

$$r_{pm} = r_0 - x_p \cdot \sin\alpha_m = r_0 - x_p \cdot m \cdot \sin\Delta \approx r_0 \qquad (5.1)$$

The matrix coefficient of equation (2.12) $HRR(p,q,k,l)$ and $HRI(p,q,k,l)$ become

$$HRR(p,q,k,l) = \frac{1}{r_0^4} \frac{\sin\left\{\frac{\omega}{a_0} L(q-l)\frac{\sin\alpha_N}{2}\right\}}{\frac{\omega}{a_0} L(q-l)\frac{\sin\alpha_N}{2}} \cdot \frac{\sin\left\{\frac{\omega}{a_0} L(p-k)\frac{\sin\alpha_M}{2}\right\}}{\frac{\omega}{a_0} L(p-k)\frac{\sin\alpha_M}{2}} \cdot \cos\frac{\omega}{a_0} L\left\{(q-l)\frac{\sin\alpha_N}{2} - (p-k)\frac{\sin\alpha_M}{2}\right\}$$

$$HRI(p,q,k,l) = \frac{1}{r_0^4} \frac{\sin\left\{\frac{\omega}{a_0} L(q-l)\frac{\sin\alpha_N}{2}\right\}}{\frac{\omega}{a_0} L(q-l)\frac{\sin\alpha_N}{2}} \cdot \frac{\sin\left\{\frac{\omega}{a_0} L(p-k)\frac{\sin\alpha_M}{2}\right\}}{\frac{\omega}{a_0} L(p-k)\frac{\sin\alpha_M}{2}} \cdot \sin\frac{\omega}{a_0} L\left\{(q-l)\frac{\sin\alpha_N}{2} - (p-k)\frac{\sin\alpha_M}{2}\right\} \qquad (5.2)$$

where $\sin\alpha_N = N \cdot \sin\Delta$, $\sin\alpha_M = M \cdot \sin\Delta$.

In these equations it appears the sin X/X type terms $\left(X = \frac{\omega}{\alpha_0} L(q-l)\frac{\sin\alpha_N}{2} \text{ or } X = \frac{\omega}{\alpha_0} L(p-k)\frac{\sin\alpha_M}{2}\right)$. This type of function is called the window function. The difference of term $HRR(p,q,k,l)$ and $HRI(p,q,k,l)$ is only the last term of right hand side, cosine function in $HRR(p,q,k,l)$ and sine function in $HRI(p,q,k,l)$.

6. Results and consideration

6.1 Error Estimation

The accuracy of calculating result is estimated by RMS. (root mean square) errors of complex correlation coefficients between the calculated and specified data. There are four types of errors; real part error ($ErrbR$), imaginary part error ($ErrbI$), magnitude error ($Errbmag$) and phase error ($Errbphase$). These errors are defined as

$$ErrbR = \left\{\frac{1}{K^2} \sum_k \sum_l (\tilde{b}R_{kl} - bR_{kl})^2\right\}^{1/2}$$

$$ErrbI = \left\{\frac{1}{K^2} \sum_k \sum_l (\tilde{b}I_{kl} - bI_{kl})^2\right\}^{1/2}$$

$$Errbmag = \left\{\frac{1}{K^2} \sum_k \sum_l (\tilde{b}mag_{kl} - bmag_{kl})^2\right\}^{1/2}$$

$$Errbphase = \left\{\frac{1}{K^2} \sum_k \sum_l ((\tilde{b}phase_{kl} - bphase_{kl}) \cdot bmag)^2\right\}^{1/2} \qquad (6.1)$$

The tilde values in the right hand sides are the specified values. The phase error has the special characteristics that it becomes large at the magnitude of correlation being very small. Because the phase is calculated by the arc tangent of ratio between real part and imaginary part of the complex correlation, so at the very small correlation coefficients of sources the error of it becomes large. When the magnitude of correlation is small, however, the phase of correlation do not important to the validity of the results. Then we use the magnitude of correlation $bmag$ as the weighted function in calculating the error of phase.

6.2 Error of estimated complex correlation coefficients

In figure 2, the variation of the error $Errbmag$ to the frequency is shown for the case of microphone ar-

ray 30*30 with statistically added noise error *AddNoise*= 0 and 5%. The solid lines are the results of this method and the dashed line is the previous one[3]. The error of this method is as small as that of previous method over the 10 kHz frequency range. Especially at the *AddNoise*=5%, the magnitude lays under the 5 % error level(−26dB). But below the 10 kHz, the error becomes large compared with the previous method. These error characteristics for low frequencies are closely related to the characteristics of matrix *H*. As indicated in chapter 5, each element of matrix *H* consists with the window function and the sine or cosine function at low frequency range.

Figure 3 shows the characteristics of matrix *H*. Fig.(a) shows the variation of the condition numbers of matrix *H* with the frequency variation. The solid line which is the case of full elements of matrix *H* is very large and the level is almost equal to the peak level of reference (3) which is shown with the alternate dashed line. The large value of this condition number makes the error of complex correlation coefficients (*bR,bI*) large. But the condition number of partial elements matrix which consists only with (*HRI,HIR*) elements, *HRI,HIR* set to zero, becomes very low as shown with the dashed line even at the low frequency range. Fig. 3(b) is the variation of window functions of equation (5.2). Each line corresponds to distances between two sources, that is, $(p-k)=0,1,2,3,4$. The levels of all lines decrease with the frequency increasing. At the $(p-k)$ values being 2, 3 or 4, the levels of the window functions decrease rapidly. So it could be expected that the elements by neighborhood sources, $(p-k)=1$ make the significant influence to the characteristics of matrix *H*. Figure 3(c) shows the variation of *HRR* and *HRI* elements for the case of $(p-k)=1$ and $(q-l)=0$. The solid and the dashed lines are the *HRR* and *HRI* elements in equation (5.2) and the alternate dotted line is the matrix element of the previous method[3]. At the previous method the in-

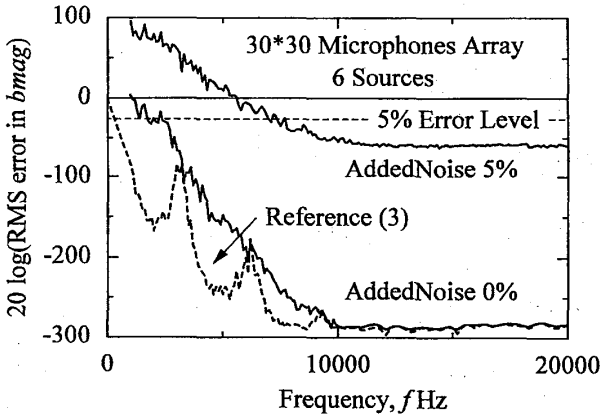

Fig. 2 Variation of rms error of *bmag* with frequency: 30*30 microphone array

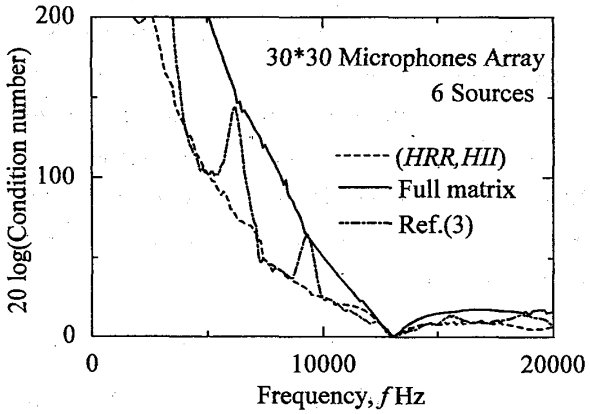

(a) Variation of condition number with frequency

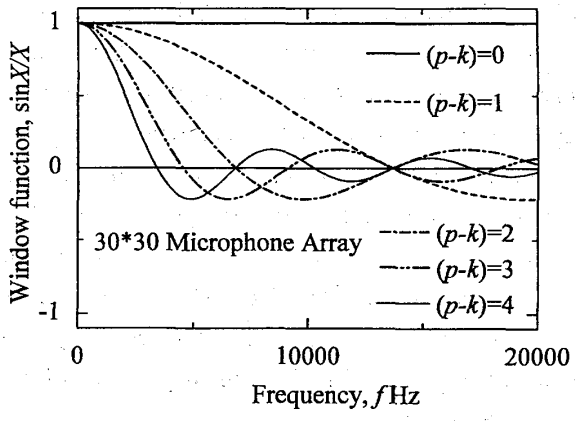

(b) Characteristics of window functions

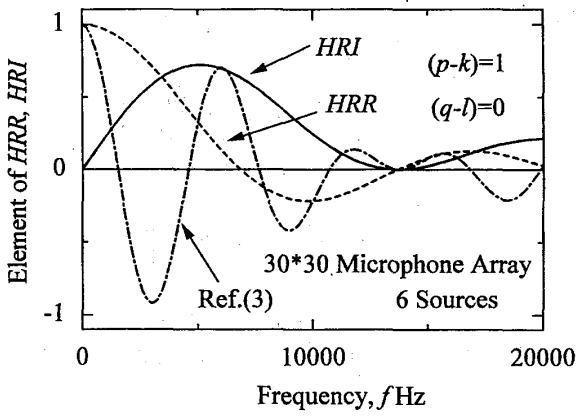

(c) Characteristics of matrix elements *HRR, HRI*

Fig. 3 Characteristics of matrix *H* 30*30 microphone array

teraction between the sound wave and the convecting disturbance generates, then the magnitude of cosine function has the periodicity. The level of it becomes large about at 3.1kHz, 6.2kHz and 9.2 kHz, and then the error of *Errbmag* becomes very large as mentioned above. But in this method, the *HRR* element (dotted line) and the *HRI* element (dashed line) have the slower periodicity. The magnitude of *HRR* gradually decreases with increasing the frequency and becomes zero at about 7kHz, but the magnitude of *HRI* becomes large nearby the frequency. So at every frequency under 10 kHz, the magnitude of *HRR* or *HRI* is large, then the matrix H becoms bad condition in this method.

Figure 4 and 5 show the error characteristics of *bR, bI* and *bphase* for *AddNoise*=0 and 5%, respectively. In both figures the error levels lay low over the 10 kHz range and becomes large below 10 kHz range. This is almost the same as the tendency of *bmag*. The level of *bR* is coincident with that of *bI* and so the phase error becomes the very small over the 10 kHz range.

Figure 6 shows the errors of *bmag* for the 6*6 microphone array. The tendency of error is almost the same as the case of 30*30 microphone array except at 13100 and 16400 Hz range. At the 13100 and 16400 Hz the cosine function of matrix *HRR* and *HII* takes the value of 2π increments with summing the microphone coherence. So all elements of *HRR* and *HII* becomes large and characteristics of matrix becomes bad. This condition is shown by reference (3), and in this method it becomes as follows from equation (2.12),

$$\frac{\omega L}{a_0}\{(k-p)\cdot m-(l-q)\cdot n\}\sin\Delta = 2\pi\cdot i$$
$$i=1,\ 2,\ 3,\ \cdots \qquad (6.2)$$

The value in the parenthesis takes only the integers. Then it is put as $(K-1)$. From this condition the frequency to reduce the accuracy is obtained as follows,

$$\frac{\omega L(K-1)}{a_0}\sin\Delta = 2\pi$$

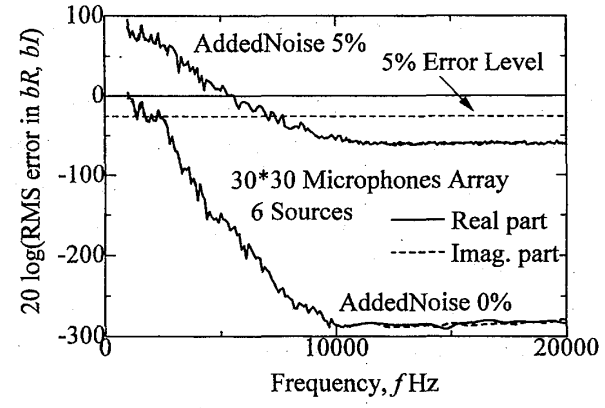

Fig. 4 Variation of rms error of *bR, bI* with frequency: 30*30 microphone array

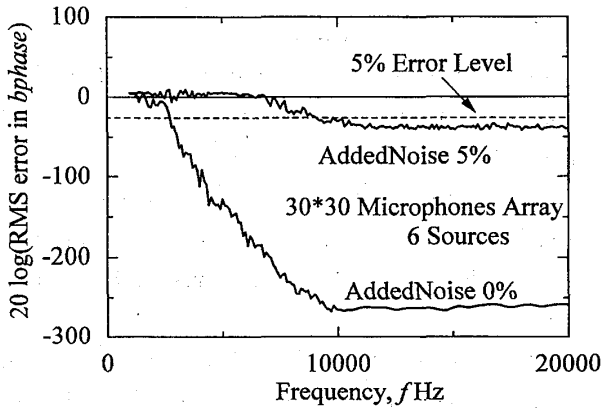

Fig. 5 Variation of rms error of *bphase* with frequency: 30*30 microphone array

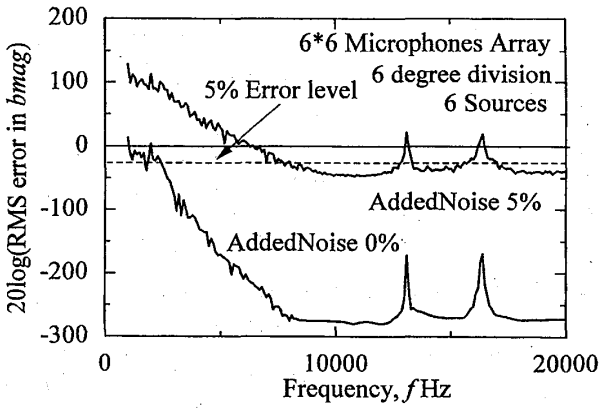

Fig. 6 Variation of rms error of *bmag* with frequency: 6*6 microphone array

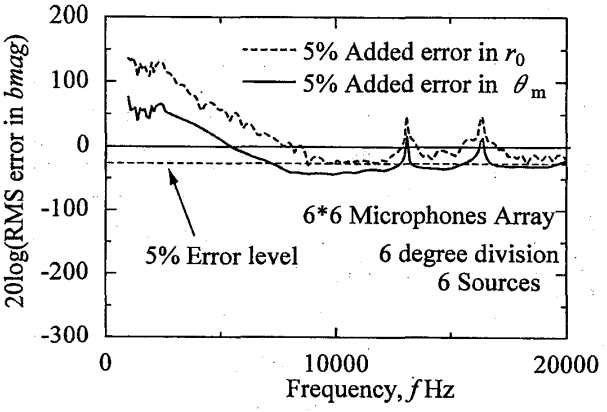

Fig. 7 Rms error of *bmag* with microphone array error in radius and angle

$$f=\frac{a_0}{L(K-1)\sin\Delta} \tag{6.3}$$

Thus at $\Delta=6$deg,$L=0.05$m the frequencies are 13100 Hz at $K=5$, 16400Hz at $K=4$, 21800Hz at $K=3$ and so on.

Figure 7 shows the influences of the microphone array errors, r_0 and θ_m errors to the correlation coefficients *bmag* for 6*6 microphone array. The error of microphone array is 5% for radius or angle positions. At the case of angle error, solid line, the level of calculated results is lower over the 10 kHz range than the 5% error level. But at the case of radius error, dashed line, the level is larger at all frequencies than the 5% error level. So it could be noticed that we have to take care of the radius positioning at setting the microphone array.

6.3 Error of estimated convecting disturbance velocity

Figure 8(a) and (b) show the errors of convecting disturbance velocity U_c for the microphone array being 30*30 and 6*6, respectively. At the case of 30*30 array of figure (a) the error levels U_c with *AddNoise*= 0% and 5% are adequately low over the 10 kHz frequency range in corresponding to the results of complex correlation coefficients. This indicates the convecting disturbance velocity U_c can be calculated at good accuracy by this method. At the case of 6*6 array of figure (b) the level at *AddNoise*=0% is almost the same as in figure (a). But the level at *AddNoise*= 5% is different from that in figure (a), that is, the level of error is over the 5% error level (dashed line) with wide frequency range. So it needs more microphones to get the accurate convecting disturbance velocity U_c.

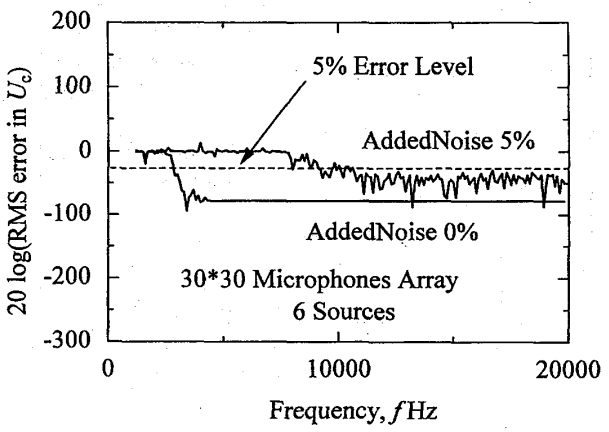

(a) 30*30 microphone array

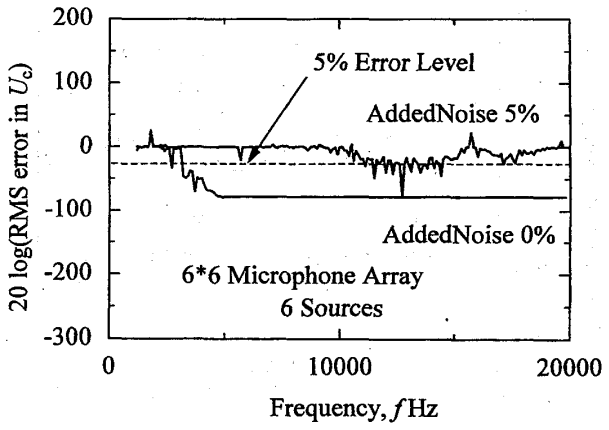

(b) 6*6 microphone array

Fig. 8 Rms error of convecting disturbance velocity

7. Conclusions

It proposed the method to estimate the complex correlation coefficients in partially coherent and the convecting disturbance velocity. We get the following results.

1) It is shown the Least Squares Fit method to find the complex correlation coefficients with good accuracy.

2) The sine terms of matrix *HIR* and *HIR* make the condition number H large and the accuracy of complex correlation coefficients bad at less than 10 kHz frequency range because of the large values of window function.

3) At the 6*6 microphone array some frequencies that the accuracy of estimated coefficients is bad exist even over 10 kHz.

4) It is shown the method to find the convecting disturbance velocity with good accuracy.

References

(1) M.J. Fisher et al," Jet Engine Source Location: The Polar Correlation Technique.", Jour. Sound and Vib., 51(1977), pp. 23–54.

(2) M.J. Fisher and K.R. Holland,"Near Field Noise Prediction Requirements", ISVR Technical Report, No. 234(1994), University of Southampton.

(3) M.J. Fisher and K.R. Holland,"Measuring relative strengths of a set of partially coherent sources", ISVR Technical Report, No. 254(1996), University of Southampton.